




Original Article

Peripapillary vessel density changes in Leber's hereditary optic neuropathy: a new biomarker

Nicole Balducci MD,¹  Maria Lucia Cascavilla MD,² Antonio Ciardella MD,³ Chiara La Morgia MD,^{4,5} Giacinto Triolo MD,² Vincenzo Parisi MD,⁶ Francesco Bandello MD,² Alfredo A Sadun MD PhD,⁷ Valerio Carelli MD PhD^{4,5} and Piero Barboni MD^{1,2}

¹Studio Oculistico d'Azeglio, ³Ophthalmology Unit, Policlinco Sant'Orsola-Malpighi, ⁴Unit of Neurology, Department of Biomedical and Neuromotor Sciences (DIBINEM), University of Bologna, ⁵IRCCS, Istituto delle Scienze Neurologiche di Bologna, Ospedale Bellaria, Bologna, ²Scientific Institute San Raffaele, Milan, ⁶GB Bietti Foundation IRCCS, Rome, Italy; and ⁷Department of Ophthalmology, Doheny Eye Institute, University of California, Los Angeles, California, USA

ABSTRACT

Importance: The contribution of the microvascular supply to the pathogenesis of Leber's hereditary optic neuropathy (LHON) is poorly understood.

Background: We aimed at measuring the peripapillary capillary vessel density (VD) using optical coherence tomography angiography (OCT-A) at different stages of LHON.

Design: Prospective, cross-sectional, multicenter, observational study.

Participants: Twenty-two LHON patients divided in four groups: unaffected mutation carriers (LHON-u); early sub-acute stage (LHON-e); late sub-acute stage (LHON-l); chronic stage (LHON-ch).

Methods: OCT-A scans centred on the optic disc were obtained by spectral domain OCT system.

Main Outcome Measures: VD, retinal nerve fibre layer (RNFL) and ganglion cell-inner plexiform layer (GC-IPL) thickness were compared between groups.

Results: Significant VD changes were detected in every sector ($P < 0.0001$). In LHON-e, the VD was reduced in the temporal sector compared with LHON-u and in the temporal and inferotemporal sectors compared with controls. In LHON-l, VD was reduced in whole, temporal, superotemporal and

inferotemporal sectors compared with LHON-u and controls. In LHON-ch, the VD was reduced in all sectors compared to the other groups. An asynchronous pattern emerged in the temporal sector with VD changes occurring earlier than RNFL thickness changes and together with GC-IPL thinning.

Conclusions and Relevance: Significant peripapillary microvascular changes were detected over the different stages of LHON. Studying the vascular network separately from fibres revealed that microvascular changes in the temporal sector preceded the changes of RNFL and mirrored the GC-IPL changes. Measurements of the peripapillary vascular network may become a useful biomarker to monitor the disease process, evaluate therapeutic efficacy and elucidate pathophysiology.

Key words: Leber hereditary optic atrophy, OCT-A, optical coherence tomography angiography, optic nerve.

INTRODUCTION

Leber's Hereditary Optic Neuropathy (LHON) is a mitochondrial disease caused by maternally inherited mitochondrial DNA (mtDNA) point mutations affecting complex I subunit genes.^{1,2} Individuals carrying the mtDNA mutation may remain asymptomatic throughout life (unaffected carrier) or suffer sudden central visual loss that rapidly worsens over

■ **Correspondence:** Dr Nicole Balducci, Studio Oculistico d'Azeglio, Piazza Galileo, 6 40123 Bologna, Italy. Email: balduccinicole@gmail.com

Received 25 January 2018; accepted 16 May 2018.

Conflict of interest: None declared.

Funding sources: The contribution of GB Bietti Foundation IRCCS was supported by the Italian Ministry of Health and Fondazione Roma.

several weeks (sub-acute stage). The sub-acute stage is characterized by a progressive evolution of the retinal nerve fibre layer (RNFL) swelling that continues for about 3 months and follows a specific pattern of thickening and subsequent thinning.³ The resulting impairment of central vision is evidenced by a central scotoma that enlarges over a few months and usually becomes a stable defect within 6 months. Minor RNFL thinning occurs after approximately 6 months from symptom presentation (dynamic stage) and the transition to the chronic stage occurs after 12 months.

Optic disc microangiopathy, characterized by an increase in tortuosity and size of the capillaries, has been described as a typical ophthalmoscopic feature that accompanies the optic disc swelling in asymptomatic and acute stage of the disease.^{4–7} For this reason the disease has been previously defined as a neurovascular disorder. However, the role of microvascular supply in the pathogenesis of LHON remains poorly understood. In particular, there remains the question as to whether these vascular features in LHON represent an epiphenomenon accompanying the pathogenic mechanism that affects the retinal ganglion cells and their axons, or, on the contrary, if the microangiopathy plays an active role in promoting the catastrophic wave of cell death that characterizes the sub-acute stage of the disease.⁸

Optical coherence tomography angiography (OCT-A) is a new, non-invasive tool available to evaluate optic nerve head vessels and radial peripapillary capillaries (RPC). Using the split-spectrum amplitude-decorrelation angiography (SSADA) algorithm, vascular perfusion can be quantified.⁹ OCT-A has been used to detect microvasculature reduction in other optic neuropathies.^{10–15} To date, only single case reports have qualitatively described microvascular changes in LHON detected by OCT-A.^{16–20}

The purpose of this study was to measure RPC vessel density (VD) in LHON patients, evaluated at different stages of the disease in order to characterize the timing and quantify the microvascular changes. Moreover, VD was compared with RNFL thickness to analyse the relationship between microangiopathy and fibre thickness changes.

METHODS

This was a prospective, cross-sectional, multicenter, observational study. The patients included had a molecularly confirmed diagnosis of LHON and were evaluated between December 2014 and September 2016 at the Sant'Orsola-Malpighi Hospital, Bologna or at the San Raffaele Scientific Institute, Milan. A control group was recruited matching the LHON patients for age and axial length (AL). As LHON predominantly affects men, only male LHON patients and controls were analysed.

All subjects had an extensive ophthalmologic examination and the following data were collected: best corrected visual acuity (BCVA), AL (Aladdin, Topcon Europe, Visia Imaging, San Giovanni Valdarno, Arezzo, Italy), intraocular pressure (IOP), mean deviation (MD) of visual field (SITA standard 30–2, Humphrey VF analyser, HFA II 750–4.1 2005; Carl Zeiss Meditec, Dublin, CA, USA), peripapillary RNFL thickness and macular ganglion cell inner plexiform layer (GC-IPL) thickness (Cirrus HD-OCT, software V.6.0; Carl Zeiss Meditec, Inc., Dublin, CA, USA) and RPC VD (OCT-A, AngioVue Imaging System; Optovue, Inc., software version 2015.100.0.33 Fremont, CA, USA).

Exclusion criteria for LHON patients were: female sex, the presence of spherical or cylindrical refractive errors higher than 4 and 2 diopters (D), respectively and the presence of any systemic or ocular pathology and/or optic nerve disease which could interfere with OCT interpretation. If both eyes of LHON patients matched the inclusion criteria, they were both analysed.

Inclusion criteria for control group were the following: male sex, BCVA of at least 0.8 (decimal fraction); spherical or cylindrical refractive errors less than 4 and 2 diopters (D), respectively; intraocular lens pressure (IOP) < 21 mmHg; normal appearance of the optic disc; normal visual field and no any ocular or systemic disease that could interfere with OCT-A examination and interpretation.

Patients were divided into four groups based on symptom duration: (i) patients carrying LHON mutation without symptoms or signs (unaffected mutation carrier LHON, LHON-u); (ii) patients in the early sub-acute stage of disease with symptom duration <3 months (early sub-acute LHON, LHON-e); (iii) patients in the late sub-acute stage of disease with symptom presentation in the previous 4–6 months (late sub-acute LHON, LHON-l); (iv) patients in the chronic stage of the disease >12 months (chronic LHON, LHON-ch).

All the participants gave their informed consent according to the Declaration of Helsinki. The internal review board at the Department of Neurological Sciences, University of Bologna, approved the study.

Average and sectorial (superior, temporal, inferior, nasal) peripapillary RNFL thickness were measured as previously described.³

OCT-A instrumentation and procedure

OCT-A scans of the optic disc and the paripapillary region were obtained by spectral domain OCT system, as already documented.¹⁴

Vascular retinal layers were visualized and segmented. The software calculates RPC VD as previously described.²¹ Briefly, RPC VDs were calculated from the superficial peripapillary retinal layers of the RPC

segment, which extend from ILM to RNFL posterior boundary. This setting is utilized to evaluate superficial peripapillary vessels, running parallel to RNFL and radial to optic nerve head and supplied by the central retinal artery (Fig. 1-left). The peripapillary region is defined as a 0.75 mm wide elliptical annulus extending from the optic disc boundary and was divided into six sectors based on the Garway-Heath map²² (Fig. 1-right). RPC VD was defined as the percentage area occupied by the large vessels and microvasculature in the peripapillary region.

Whole and sectorial VDs were analysed. Two investigators (N.B. and P.B.) checked segmentation and image quality before testing VD.

The datasets generated during and/or analysed during the current study are available from the corresponding author upon request.

Statistical analysis

Values were presented as mean \pm standard deviation (SD). BCVA was converted into the logarithm of the minimum angle of resolution (LogMAR) units for the statistical analysis.

Data passed the normality test so the analysis of variance (ANOVA) test was used for comparisons between groups, followed by Bonferroni post-hoc test for pair wise comparisons.

In order to compare VD and RNFL changes, we first merged the superonasal with the superotemporal VD and the inferonasal with the inferotemporal VD, so two sectors were obtained: superior and inferior, respectively. Then, as RPC VD is the percentage of area occupied by vessels in the RNFL volume, sectorial VD was normalized for corresponding sectorial RNFL thickness obtaining vascular thickness values (which we called 'normalized VD') using the following formula: (sectorial RPC VD * sectorial RNFL thickness)/100.

Statistical significance was assumed for P values < 0.05 . GraphPad InStat (V.3a) for Macintosh (GraphPad Software, San Diego, CA, USA) was used for statistical analysis.

RESULTS

Twenty-two male LHON patients were enrolled as follows: eight patients (15 eyes) in the LHON-u group; four patients (eight eyes) in the LHON-e group; five patients (10 eyes) in the LHON-l group and nine patients (16 eyes) in the LHON-ch group. The four patients in the LHON-e group were also included in the LHON-l group, as they were examined twice during their sub-acute (LHON-e and LHON-l) stage of the disease, and were counted each time. Three eyes of three patients were excluded from statistical analysis for poor quality images due to motion artefacts. Thirteen patients carried the mtDNA mutation m.11778G>A/MT-ND4 gene, five patients carried the m.3460G>A/MT-ND1, two patients carried the m.14258G>A/MT-ND6, one patient carried the m.14484T>C/MT-ND6 and one patient carried the m.15222A>G/MT-CTB.

Eight male subjects (eight eyes) were enrolled in the control group. Clinical data from all the groups are summarized in Table 1.

Vessel density analysis

A series of changes characterized the microvascular network as detected during disease progression from LHON-u to LHON-ch stages, through the transition of LHON-e and LHON-l, as shown in Figure 2.

Table 2 summarizes mean \pm SD of RPC VD in each sector in LHON groups and controls. ANOVA was statistically significant in every sector analysed ($P < 0.0001$).

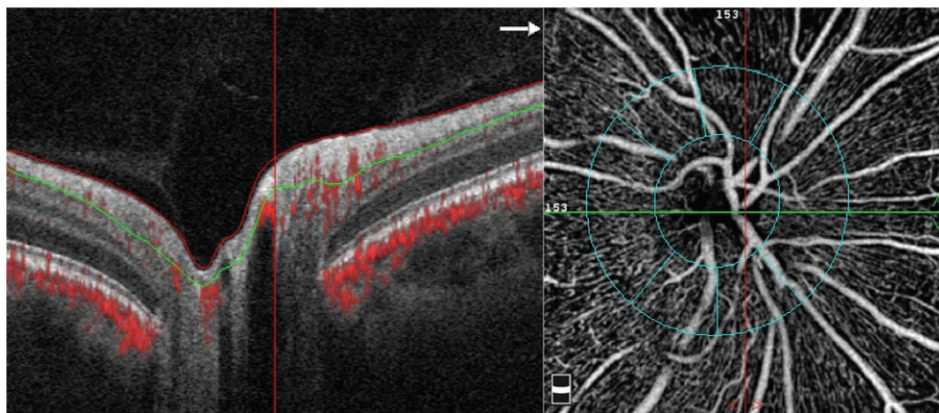


Figure 1. Vascular retinal layers segmentation. Optical coherence tomography (OCT, left) and optical coherence tomography angiography (OCT-A, right) of a control right eye. Note the layer segmentation (green line, OCT image) which follows the posterior boundary of the retinal nerve fibre layer and the visualization of the radial peripapillary capillaries (RPC) with OCT-A. Note the blue circles superimposed to the optic nerve head, representing the optic nerve boundary (inner circle) and the peripapillary sectors (outer circle): temporal, superotemporal, superonasal, nasal, inferonasal, inferotemporal.

No statistically significant differences of VD were found between LHON-u and controls in any sector.

In LHON-e stage the VD was significantly reduced in the temporal sector compared with LHON-u and in the temporal and inferotemporal sectors compared with controls.

In LHON-l stage VD was significantly reduced in whole, temporal, superotemporal and inferotemporal sectors compared with LHON-u and controls.

In LHON-ch stage, the VD was reduced in all sectors when compared to all the other stages, including the control group.

Table 3 shows the percentage of VD and RNFL thickness changes of LHON groups in each sector compared to the control group. Moreover, Table 3 shows also the percentage of nasal (average values of inferonasal and superonasal macular sectors, which correspond to temporal VD sector) GC-IPL thickness changes respect to controls.

Considering the LHON-u, there was a slight, but not statistically significant, increase of temporal VD (+2.1% respect to controls), at odds with the other sectors, whereas the RNFL was increased in all sectors (+11.4%, +3.7%, 1.9%, 11.1% respect to controls for the temporal, superior, nasal and inferior sectors, respectively). In the transition to LHON-e, VD became reduced in all sectors except for the

superonasal, which was increased, whereas RNFL was increased in all sectors. Subsequently, in the transition to LHON-l VD displayed the same pattern of reduction, whereas the RNFL temporal sector started to be reduced. Finally, in the LHON-ch the VD and RNFL were greatly reduced in all sectors.

Table 4 shows the normalized VD changes respect to controls. Changes of RNFL thickness, nasal GC-IPL thickness and normalized VD through the different stages of disease, as compared to Controls, are summarized in the graph and depicted in Figure 3.

This analysis revealed an asynchronous pattern of changes in temporal VD and RNFL thickness, in contrast to the remaining sectors, where a more synchronous increase/decrease of VD and RNFL thickness was observed. In fact, temporal VD and RNFL appeared to be both increased in LHON-u and at conversion to LHON-e. Subsequently, evolving into LHON-l, VD was rapidly reduced as opposed to a delayed thinning of RNFL in this sector. Temporal VD and nasal GC-IPL thickness showed similar early reduction.

DISCUSSION

This study reveals significant peripapillary microvascular changes over the different stages of disease progression in patients affected by LHON. The

Table 1. Clinical data derived from LHON patients at different stages and controls

	LHON-u	LHON-e	LHON-l	LHON-ch	Controls	P value ^{§§§}
Eyes (number)	15	8	10	16	8	
Age (years)	21.38 ± 9.9XX	28.75 ± 15.64	29 ± 13.6	33.22 ± 10.69	32 ± 6.16	ns
Genotype mutation (number of eyes)	11778G>A (6) 3460G>A (7) 14258G>A (2)	11778G>A (6) 3460G>A (2)	11778G>A (8) 3460G>A (2)	11778G>A (11) 14258G>A (2) 15222A>G (2) 14 484T>C (1)	–	
BCVA (LogMAR)	–0.02 ± 0.01	0.95 ± 0.73	1.26 ± 0.46	0.95 ± 0.6	–0.03 ± 0.02	<0.0001
MD (dB)		–6.0 ± 6.1		–13.14 ± 7.87		<0.0001
RNFL av	105.53 ± 9.24 [†]	115 ± 11.82 [†]	109.87 ± 9.12 [†]	67.88 ± 13.55	97.79 ± 7.43 [‡]	<0.0001
RNFL t	76.13 ± 7.09 ^{†,§}	71 ± 16.66 [‡]	55.5 ± 11.95	44.5 ± 11.03	68.33 ± 10.75 [†]	<0.0001
RNFL s	128.13 ± 17.10 [†]	144.3 ± 19.13 [†]	144.5 ± 15.54 [†]	81.61 ± 19.69	123.5 ± 13.83 [†]	<0.0001
RNFL i	140.2 ± 16.38 [†]	159.6 ± 17.39 ^{†,¶}	152.8 ± 20.53 [†]	79.17 ± 17.78	126.2 ± 13.17 ^{††}	<0.0001
RNFL n	74.8 ± 12.61 ^{††}	82.88 ± 10.66 [‡]	87.13 ± 11.99 [†]	61.44 ± 10.91	73.39 ± 11.09	<0.0001
GC-IPL av	84.93 ± 4.8 ^{†,‡‡}	68.14 ± 9.11	59.75 ± 5.36	51.61 ± 6.07	84.52 ± 6.03 ^{†,§§}	<0.0001
GC-IPL in	84.6 ± 4.8 ^{¶¶,†††,†}	63.5 ± 8.15 ^{†,‡‡‡}	56 ± 4.78 ^{‡‡‡}	49.01 ± 5.29 ^{‡‡‡}	84.21 ± 6.25	<0.0001
GC-IPL sn	86.26 ± 5.58 ^{¶¶,†††,†}	65.37 ± 11.32 ^{†,‡‡‡}	58.12 ± 6.4 ^{‡‡‡}	50.43 ± 6.04 ^{‡‡‡}	85.91 ± 5.98	<0.0001
GC-IPL s	86.8 ± 5.75 ^{¶¶,†††,†}	72.62 ± 10.58 ^{†,‡‡‡}	62.75 ± 7.45 ^{‡,‡‡‡}	51.43 ± 7.16 ^{‡‡‡}	85.3 ± 6.18	<0.0001
GC-IPL st	84.8 ± 5.33 ^{¶¶,†††,†}	69.75 ± 10.58 ^{†,‡‡‡}	63.5 ± 6.9 ^{†,‡‡‡}	50.43 ± 6.09 ^{‡‡‡}	84.69 ± 6.8	<0.0001
GC-IPL-it	86.6 ± 4.13 ^{¶¶,†††,†}	67.12 ± 8.42 ^{†,‡‡‡}	62.5 ± 6.48 ^{†,‡‡‡}	52 ± 4.85 ^{‡‡‡}	83.69 ± 6.11	<0.0001
GC-IPL i	83.2 ± 4.36 ^{¶¶,†††,†}	65.25 ± 9.99 ^{†,‡‡‡}	61.5 ± 7.15 ^{††,‡‡‡}	51.87 ± 6.26 ^{‡‡‡}	83.69 ± 6.76	<0.0001
AL (mm)	24.64 ± 1.23	23.15 ± 0.06	22.34 ± 0.9	22.77 ± 0.65	23.87 ± 0.82	ns

[†]Bonferroni post-hoc test $P < 0.001$ versus LHON-ch. [‡]Bonferroni post-hoc test $P < 0.01$ versus LHON-ch. [§]Bonferroni post-hoc test $P < 0.05$ versus LHON-l. [¶]Bonferroni post-hoc test $P < 0.05$ versus control. ^{††}Bonferroni post-hoc test $P < 0.05$ versus LHON-ch. ^{‡‡}Bonferroni post-hoc test $P < 0.01$ versus LHON-l. ^{§§}Bonferroni post-hoc test $P < 0.01$ versus LHON-l. ^{¶¶}Bonferroni post-hoc test $P < 0.001$ versus LHON-e. ^{†††}Bonferroni post-hoc test $P < 0.001$ versus LHON-l. ^{‡‡‡}Bonferroni post-hoc test $P < 0.001$ versus control. ^{§§§}ANOVA. AL, axial length; av., average; BCVA, best-corrected visual acuity; ch, chronic; dB, decibel; e, early phase (between 1 and 2 months); GC-IPL, macular ganglion cell-inner plexiform layer; i, inferior; l, late phase (between 4 and 6 months); LHON, Leber hereditary optic neuropathy; LogMAR, logarithm of the minimum angle of resolution; MD, mean defect; n, nasal; RNFL, ns, not significant; retinal nerve fibre layer; s, superior; t, temporal; u, unaffected carrier.

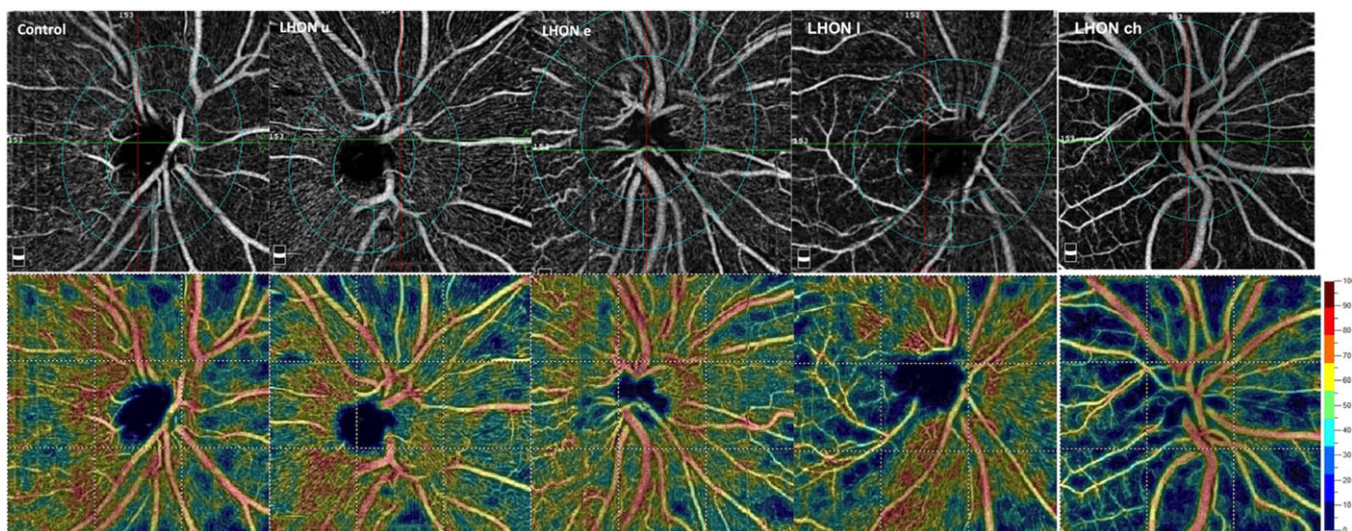


Figure 2. Example of OCT-A in the different groups. Vascular visualization of radial peripapillary capillaries (RPC, upper images) layers in the five groups analysed (control; LHON-u: unaffected carrier; LHON-e: early acute stage; LHON-l: late acute stage; LHON-ch: chronic stage). Note the progressive reduction in vessel density as the disease advances, as displayed in the density maps (bottom images; color code: blue color indicates low vessel density).

changing pattern of RNFL and GC-IPL is consistent with previous works.^{3,23} The key finding is that microvascular changes in the temporal sector, implicating the papillomacular bundle, precede the RNFL and mirror the GC-IPL changes. This argues in favour of an active role played by the retinal microvasculature in the process of disease during LHON conversion that leads to an irreversible wave of axonal injury (RNFL thickening) and an irreversible wave of retinal ganglion cells (RGC) loss (GC-IPL thinning). At late chronic stage a generalized thinning affects retinal microvasculature, RNFL and GC-IPL.

Optic disc microangiopathy is a hallmark of LHON, seen both in asymptomatic carriers and in the symptomatic stage of disease, affecting mostly the temporal region.^{4-7,24}

We failed to find any VD differences between LHON-u and controls in all sectors analysed. However, when VD was normalized for RNFL thickness,

the vascular network in the temporal sectors was increased in LHON-u (Table 4). After conversion, VD was reduced prior to the reduction of RNFL thickness.³ Relevantly, in parallel to VD reduction also GC-IPL was reduced during the LHON-e sub-acute stage. This pattern highlights that even if a parallel sequence of events occurs, VD and RNFL changes are not simultaneous in the temporal sector, which represents the papillomacular region. Remarkably, VD and GC-IPL instead seem to follow the same rate of reduction suggesting a tighter link of VD with RGCs than with their axons, clearly evident in the area where the pathological mechanism hits first. In the other sectors a more synchronous increase/decrease of VD and RNFL thickness was observed.

An explanatory hypothesis on the critical role of the vascular component in the LHON pathogenic mechanisms, requires consideration of two key questions:

Table 2. Vessel density (VD) in LHON patients at different stages and in control

VD (%)	LHON-u	LHON-e	LHON-l	LHON-ch	Control	P value [†]
Whole RPC	62.27 ± 2.2 ^{¶,††}	59.2 ± 4.3 ^{††}	56.68 ± 3.2 ^{‡,††,‡‡}	46.92 ± 4.4 ^{‡,§,¶,‡‡}	63.11 ± 2.9 ^{¶,††}	<0.0001
RPC-N	58.15 ± 4.0 ^{††}	59.33 ± 4.11 ^{††}	58.75 ± 3.8 ^{††}	48.57 ± 5.4 ^{‡,§,¶,‡‡}	60.35 ± 3.65 ^{††}	<0.0001
RPC-IN	62.69 ± 4.8 ^{††}	67.09 ± 5.4 ^{††}	60.9 ± 4.8 ^{††}	49.19 ± 8.7 ^{‡,§,¶,‡‡}	64 ± 4.6 ^{††}	<0.0001
RPC-IT	65.30 ± 4.0 ^{¶,††}	62.16 ± 5.4 ^{††,‡‡}	58.47 ± 4.21 ^{‡,††,‡‡}	47.9 ± 6.6 ^{‡,§,¶,‡‡}	67.87 ± 3.9 ^{¶,††}	<0.0001
RPC-ST	66.40 ± 2.8 ^{¶,††}	62.7 ± 7.8 ^{††}	56.33 ± 6.3 ^{‡,††,‡‡}	49.08 ± 8.9 ^{‡,§,¶,‡‡}	66.42 ± 4.24 ^{¶,††}	<0.0001
RPC-SN	59.23 ± 5.5 ^{††}	62.35 ± 2.85 ^{††}	60.7 ± 4.74 ^{††}	48.14 ± 8.1 ^{‡,§,¶,‡‡}	59.74 ± 5.13 ^{††}	<0.0001
RPC-T	65.23 ± 3.3 ^{h,§,¶}	52.81 ± 5.9 ^{‡,††,‡‡}	49.54 ± 4.39 ^{‡,††,‡‡}	41.69 ± 4.2 ^{‡,§,¶,‡‡}	63.89 ± 3.59 ^{§,¶,††}	<0.0001

[†]ANOVA. [‡]Bonferroni post-hoc test statistically significant versus LHON-u. [§]Bonferroni post-hoc test statistically significant versus LHON-e. [¶]Bonferroni post-hoc test statistically significant versus LHON-l. ^{††}Bonferroni post-hoc test statistically significant versus LHON-ch. ^{‡‡}Bonferroni post-hoc test statistically significant versus control. ch, chronic stage; e, early acute stage; IN, inferonasal; IT, inferotemporal; l, late acute stage; LHON, Leber hereditary optic neuropathy; N, nasal; RPC, radial peripapillary capillaries; SN, superonasal; ST, superotemporal; T, temporal; u, unaffected carrier; VD, vessel density.

Table 3. Percentage (%) of vessel density (VD), retinal nerve fibre layer (RNFL) and macular ganglion cells-inner plexiform layer (GC-IPL) thickness changes respect to controls

Sector	LHON-u	LHON-e	LHON-l	LHON-ch
Whole RPC	-1.3	-6.2	-10.2	-25.7
RPC-T	2.1	-17.3	-22.5	-34.7
RPC-ST	0.0	-5.6	-15.2	-26.1
RPC-SN	-0.9	4.4	1.6	-19.4
RPC-N	-3.6	-1.7	-2.7	-19.5
RPC-IN	-2.0	-1.4	-4.8	-23.1
RPC-IT	-3.8	-8.4	-13.9	-29.4
RNFL Avg	7.9	17.6	12.4	-30.6
RNFL t	11.4	3.9	-18.8	-34.9
RNFL s	3.7	16.8	17.0	-33.9
RNFL n	1.9	12.9	18.7	-16.3
RNFL i	11.1	26.5	21.1	-37.3
GC-IPL-N [†]	0.44	-24.24	-32.91	-44.95

[†]Average values of inferonasal and superonasal sectors. ch, chronic stage; e, early acute stage; IN, inferonasal; IT, infero-temporal; l, late acute stage; LHON, Leber hereditary optic neuropathy; N, nasal; RNFL, retinal nerve fibre layer; SN, superonasal; ST, superotemporal; T, temporal; u, unaffected carrier.

1. Why does temporal vessel density increase during the RNFL swelling (LHON-u to pre-conversion stage)?

The metabolic consequences of RGC mitochondrial impairment likely results in axonal transport stasis and swelling, which in turn may produce a stress signalling leading to a local 'reactive' microangiopathy, primarily affecting the area of the papillomacular bundle, where a compensatory vascular response possibly develops. This condition may remain in equilibrium, waxing and waning for years, and produces the characteristic fundus changes described in unaffected LHON carriers.^{24,25} However, after conversion to the sub-acute stage of the disease, the microvascular changes decrease in the temporal sector paralleling RGCs loss, while temporal RNFL tends to remain asynchronously thick, as quantified by VD at OCT measurements in the present study. The relationship between RPC VD and RNFL thickness has been recently studied, suggesting a non-linear correlation.²⁶ Specifically, an almost linear relationship between

increase of RNFL thickness and RPC VD is lost when RNFL thickness crosses a threshold over which there is no further increment of VD.²⁶ However, to fully understand what triggers the disease conversion we currently still lack a longitudinal follow-up study of multiple patients in the pre-clinical stage immediately preceding the visual loss. A qualitative study of one single patient in the early sub-acute stage (10 days after visual symptoms onset) in one eye and in the pre-symptomatic stage in the other eye found dilated peripapillary microvasculature in the temporal side of the optic disc.²⁰ The authors hypothesized that dilated peripapillary capillaries may derive from a vasodilating signalling due to RNFL shortage of ATP.

Differently, another recent case report qualitatively analysed longitudinal changes in RPC in correlation to RNFL in a patient followed from the acute and presymptomatic stages in the two eyes, respectively.¹⁹ These authors concluded that temporal RPC defects start to spread once the pseudoe-dema begins to resolve. Our current results link tightly the loss of RPC to that of RGCs at LHON-e stage, when RNFL is still thick and thickness reduction proceeds at slower rate.

2. Why does the temporal vessel density decrease before the loss of fibres noted in the progression to the sub-acute stage?

Our current results, linking in a parallel fashion the decrease of VD and RGCs, as exemplified by GC-IPL thinning, strongly suggest a metabolic relation between RGCs soma and vascular supply. The persistence of axonal swelling, which most probably relates to a stasis of organellar transport, resolves at a slower rate. Lacking a longitudinal follow-up at the crucial transition from pre-clinical to conversion, we can only speculate on what triggers conversion and we cannot exclude that the VD reduction is only a consequence of optic nerve atrophy, similarly to other chronic optic neuropathy.¹⁰⁻¹⁸ However, one hypothesis to explain the catastrophic rapidity of disease onset, which occurs in days to weeks may implicate some anatomical considerations. The laminar portion of the optic nerve is limited in being

Table 4. Percentage (%) of no-normalized and normalized vessel density (averaged in four sectors) changes respect to controls

Parameter	Sector	LHON-u	LHON-e	LHON-l	LHON-ch
VD	RPC-T	2.1	-17.3	-22.5	-34.7
%(%)	RPC-S	-0.4	-0.9	-7.2	-22.9
	RPC-N	-3.6	-1.7	-2.7	-19.5
	RPC-I	-2.9	-5.0	-9.5	-26.4
Normalized VD microns (%)	RPC-T	13.8	-14.1	-37.0	-57.5
	RPC-S	3.3	15.8	8.5	-49.1
	RPC-N	-1.8	11.0	15.6	-32.6
	RPC-I	7.8	20.1	9.6	-53.8

ch, chronic stage; e, early acute stage; l, inferior; l, late acute stage; N, nasal; RPC, radial peripapillary capillaries; S, superior; T, temporal; u, unaffected carriers; VD, vessel density.

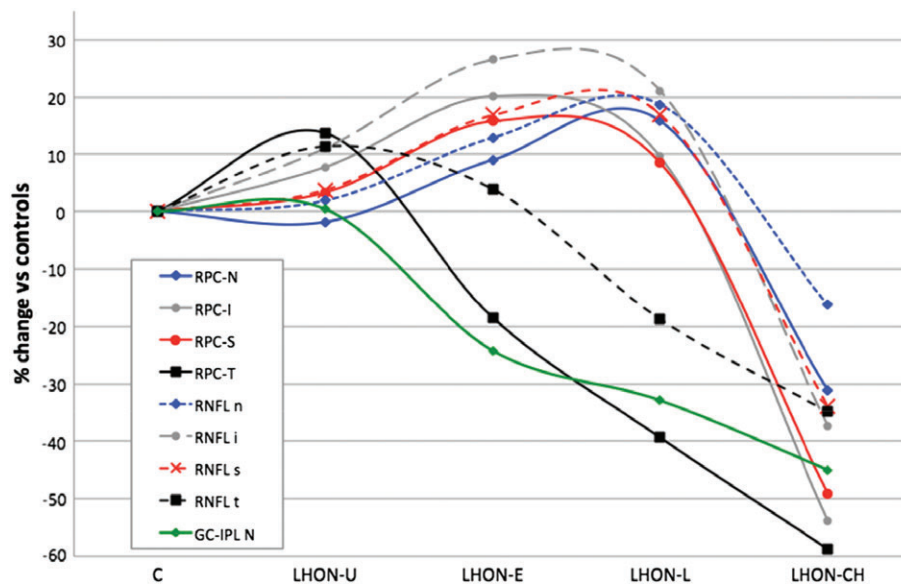


Figure 3. Changes respect to controls of retinal nerve fibre layer (RNFL) thickness, nasal ganglion cells-inner plexiform layer (GC-IPL) thickness and normalized vessel density (VD) in Leber's hereditary optic neuropathy (LHON) patients at different stage of the disease. Dotted lines indicate RNFL values in the different quadrants, whereas solid lines indicate measurements corresponding to normalized VD of different radial peripapillary capillaries (RPC) sectors. Green line represents nasal (average values of inferonasal and superonasal sectors) GC-IPL changes. Data are reported as percentage of change from the average value of healthy controls. C, controls; U, unaffected carriers; E, early acute stage; L, late acute stage; CH, chronic stage; RPC, radial peripapillary capillaries; N, nasal; I, inferior; S, superior; T, temporal; RNFL, retinal nerve fibre layer; GC-IPL, ganglion cells-inner plexiform layer.

able to anatomically accommodate axonal swelling and this may lead to some extent a compartment issue. A mechanical component may be envisaged, in which mounting swelling of axons entering the optic nerve head raises post-laminar tissue pressure. Relevantly, small discs are a risk factor in LHON.²⁷ In this scenario, the insufficiency of vascular supply occurring when VD reaches the plateau despite the still increasing RNFL thickness may trigger the catastrophic propagation of RGC neurodegeneration and loss, followed only at later stages by axonal loss. Thus, a mixed mechanical/metabolic mechanism may fit the hypothetical sequence of the events characterizing the LHON conversion. A small or congested disc could predispose to a metabolic recursive process that we might call a metabolic compartment syndrome. The small and most vulnerable axons crowded together, in a condition of incongruent vascular supply precipitated by decrease of VD, might, through the reiterative release of ROS, initiate a domino effect that rapidly propagates with a precise pattern.^{28,29} This sequence of events fits the current interpretation of the stroke-like events documented in mitochondrial encephalopathy, lactic acidosis, stroke-like episodes (MELAS), which is characterized by lack of true ischemia whereas cytotoxic intracellular oedema occurs.

The present results, it should be noted, do not parallel our recent findings regarding choroidal thickness changes seen in LHON.³⁰ This previous publication demonstrated that the RNFL and

choroid in LHON underwent an increase in thickness, followed by permanent thinning, and the RNFL changes preceded those affecting the choroid. The choroidal changes may simply have been a surrogate marker of RGC and axonal atrophy and a remote vascular compensatory adaptation.

The cross-sectional nature of the present study has limitations. A longitudinal study might document the dynamic changes over time, thus confirming the hypothesized scenario. However, we do have follow-up time points in a few patients in our study. Many of our patients had both eyes studied and this can be a statistical confounder, however LHON is such a rare disease that having more eyes to study was an offsetting advantage. Moreover, we did not measure VD in the macular region, and further studies will be necessary to evaluate changes of the microvasculature in order to detect if they follow or precede the GCLs changes. Another limitation is related to genetic heterogeneity of the patients studied. A meaningful stratification by mutation was thus not performed, since the 11778G>A/MT-ND4 was over-represented.

Overall, the present study allowed, for the first time, to quantify the peripapillary vascular changes seen at the different stages of LHON natural history and our findings highlight the vascular role in the pathogenesis of the disease. Measurements of vascular changes in LHON may become a useful biomarker to monitor the disease

progression, evaluate therapeutic efficacy and elucidate pathophysiology.

REFERENCES

- Carelli V, Ross-Cisneros FN, Sadun AA. Mitochondrial dysfunction as a cause of optic neuropathies. *Prog Retin Eye Res* 2004; **23**: 53–89.
- Yu-Wai-Man P, Griffiths PG, Chinnery PF. Mitochondrial optic neuropathies – disease mechanisms and therapeutic strategies. *Prog Retin Eye Res* 2011; **30**: 81–114.
- Barboni P, Carbonelli M, Savini G et al. Natural history of Leber's hereditary optic neuropathy: longitudinal analysis of the retinal nerve fiber layer by optical coherence tomography. *Ophthalmology* 2010; **117**: 623–7.
- Smith JL, Hoyt WF, Susac JO. Ocular fundus in acute Leber optic neuropathy. *Arch Ophthalmol* 1973; **90**: 349–54.
- Nikoskelainen E, Sogg RL, Rosenthal AR, Friberg TR, Dorfman LJ. The early phase in Leber hereditary optic atrophy. *Arch Ophthalmol* 1977; **95**: 969–78.
- Nikoskelainen E, Hoyt WF, Nummelin K. Ophthalmoscopic findings in Leber's hereditary optic neuropathy: I. Fundus findings in asymptomatic family members. *Arch Ophthalmol* 1982; **100**: 1597–602.
- Nikoskelainen E, Hoyt WF, Nummelin K. Ophthalmoscopic findings in Leber's hereditary optic neuropathy: II. The fundus findings in the affected family members. *Arch Ophthalmol* 1983; **101**: 1059–68.
- Carelli V, La Morgia C, Valentino ML, Barboni P, Ross-Cisneros FN, Sadun AA. Retinal ganglion cell neurodegeneration in mitochondrial inherited disorders. *Biochim Biophys Acta* 2009; **1787**: 518–28.
- Jia Y, Morrison JC, Tokayer J et al. Quantitative OCT angiography of optic nerve blood flow. *Biomed Opt Express* 2012; **3**: 3127–37.
- Liu L, Jia Y, Takusagawa HL et al. Optical coherence tomography angiography of the peripapillary retina in glaucoma. *JAMA Ophthalmol* 2015; **133**: 1045–52.
- Wang X, Jiang C, Ko T et al. Correlation between optic disc perfusion and glaucomatous severity in patients with open-angle glaucoma: an optical coherence tomography angiography study. *Graefes Arch Clin Exp Ophthalmol* 2015; **253**: 1557–64.
- Mwanza JC, Budenz DL. Optical coherence tomography platforms and parameters for glaucoma diagnosis and progression. *Curr Opin Ophthalmol* 2016; **27**: 102–10.
- Wang X, Jia Y, Spain R et al. Optical coherence tomography angiography of optic nerve head and parafovea in multiple sclerosis. *Br J Ophthalmol* 2014; **98**: 1368–73.
- Balducci N, Ciardella A, Gattergna R et al. Optical coherence tomography angiography of the peripapillary retina and optic nerve head in dominant optic atrophy. *Mitochondrion* 2017; **36**: 60–5.
- Chen JJ, AbouChehade JE, Iezzi R Jr, Leavitt JA, Kardouk RH. Optical coherence angiographic demonstration of retinal changes from chronic optic neuropathies. *Neuro-Ophthalmology* 2017; **41**: 76–83.
- De Rojas JO, Rasool N, Chen RW, Horowitz J, Odel JG. Optical coherence tomography angiography in Leber hereditary optic neuropathy. *Neurology* 2016; **87**: 2065–6.
- Takayama K, Ito Y, Kaneko H, Kataoka K, Ra E, Terasaki H. Optical coherence tomography angiography in Leber hereditary optic neuropathy. *Acta Ophthalmol* 2017; **95**: e344–5.
- Falavarjani GK, Tian JJ, Akil H, Garcia GA, Sadda SR, Sadun AA. Swept source optical coherence tomography angiography of the optic disk in optic neuropathy. *Retina* 2016; **36**: S168–77.
- Matsuzaki M, Hiramami Y, Uyama H, Kurimoto Y. Optical coherence tomography angiography changes in radial peripapillaries in Leber hereditary optic neuropathy. *Am J Ophthalmol Case Rep* 2018; **9**: 51–5.
- Gaier ED, Gittinger JW, Cestari DM, Miller JB. Peripapillary capillary dilatation in Leber hereditary optic neuropathy revealed by optical coherence tomography angiography. *JAMA Ophthalmol* 2016; **134**: 1332–4.
- Rao HL, Pradhan ZS, Weinreb RN et al. Regional comparisons of optical coherence tomography angiography vessel density in primary open angle glaucoma. *Am J Ophthalmol* 2016; **171**: 75–83.
- Garway-Heath DF, Poinosawmy D, Fitzke FW, Hitchings RA. Mapping the visual field to the optic disc in normal tension glaucoma eyes. *Ophthalmology* 2000; **107**: 1809–15.
- Balducci N, Savini G, Cascavilla ML et al. Macular nerve fibre and ganglion cell layer changes in acute Leber's hereditary optic neuropathy. *Br J Ophthalmol* 2016; **100**: 1232–7.
- Sadun F, De Negri AM, Carelli V et al. Ophthalmologic findings in a large pedigree of 11778/Haplogroup J Leber hereditary optic neuropathy. *Am J Ophthalmol* 2004; **137**: 271–7.
- Barboni P, Savini G, Feuer WJ et al. Retinal nerve fiber layer thickness variability in Leber hereditary optic neuropathy carriers. *Eur J Ophthalmol* 2012; **22**: 985–91.
- Jia Y, Simonett JM, Wang J et al. Wide-field OCT angiography investigation of the relationship between radial Peripapillary capillary plexus density and nerve fiber layer thickness. *Invest Ophthalmol Vis Sci* 2017; **58**: 5188–94.
- Ramos Cdo V, Bellusci C, Savini G et al. Association of optic disc size with development and prognosis of Leber's hereditary optic neuropathy. *Invest Ophthalmol Vis Sci* 2009; **50**: 1666–74.
- Sadun AA, Win PH, Ross-Cisneros FN, Walker SO, Carelli V. Leber's hereditary optic neuropathy differentially affects smaller axons in the optic nerve. *Trans Am Ophthalmol Soc* 2000; **98**: 223–32.
- Pan BX, Ross-Cisneros FN, Carelli V et al. Mathematically modeling the involvement of axons in Leber's hereditary optic neuropathy. *Invest Ophthalmol Vis Sci* 2012; **53**: 7608–17.
- Borrelli E, Triolo G, Cascavilla ML et al. Changes in choroidal thickness follow the RNFL changes in Leber's hereditary optic neuropathy. *Sci Rep* 2016; **6**: 37332.